

Original paper

Petrology and geochemical characteristics of phlogopite pyroxenite related to durbachites, Moldanubian Zone, Bohemian Massif

Jakub TRUBAČ^{1*}, Stanislav VRÁNA², Eva HALUZOVÁ³, Lukáš ACKERMAN³

¹ Institute of Geochemistry, Mineralogy and Mineral Resources, Charles University, Albertov 6, 128 43 Prague 2, Czech Republic; jakub.trubac@gmail.com

² Czech Geological Survey, Klárov 3, 118 21 Prague 1, Czech Republic

³ Institute of Geology v.v.i., The Czech Academy of Sciences, Rozvojová 269, 165 00 Prague 6, Czech Republic;

* Corresponding author



The phlogopite pyroxenite with a high content of pyrrhotite forms a body of circular outline about 1 km in diameter at Přední Zvonková in Moldanubian Zone (Šumava/Bohemian Forest/Böhmerwald), Czech Republic. The contours of pyroxenite body are indicated by magnetometry and gravity data. Loose blocks up to 70 cm in size scattered on fields in the flat terrain indicate that the rock is at least partly exposed at the current erosion level. The best preserved sample SV235A is a medium-grained rock containing 27 vol. % phlogopite, 23 % diopside, 25 % enstatite, abundant apatite (7 %), minor plagioclase (3 %, An_{39–42}), and pyrrhotite (3 %). Tendency to sulphide segregation is indicated by several mm pyrrhotite aggregates enclosing individual grains of pyroxenes, phlogopite and apatite.

In the *mg#* vs. MgO diagram the studied pyroxenites plot along the linear trend defined by granitoid durbachites (melanocratic quartz syenites, quartz monzodiorites to melagranites), biotite–amphibole quartz diorites and biotite–amphibole ultramafic rocks (all from the Moldanubian Zone in southern and south–central Bohemia), after the whole-rock compositions of pyroxenites are corrected for the respective content of pyrrhotite. Several pyroxene thermometers yield equilibration temperatures in the range of 970 to 1040 °C for the sample SV235A.

The Re–Os and Sr–Nd isotope composition of whole-rock samples indicates important crustal component in the sulphides and silicates. Petrological and geochemical data show a major role of fractional crystallization/crystal accumulation in formation of these rocks but magma mixing process is also recorded. The phlogopite pyroxenite is a rare rock important for understanding genesis of durbachitic magmatism.

Keywords: phlogopite pyroxenite, durbachite, cumulate, Moldanubian Zone

Received: 15 January 2015; **accepted:** 18 March 2015; **handling editor:** Emil Jelínek

1. Introduction

Amphibole–biotite/phlogopite granitoids, often with quartz syenite and quartz monzonite compositions, designated as durbachites, represent important rock-types in the Moldanubian Zone of the Variscan orogenic belt (von Raumer et al. 2014; Žák et al. 2014; Tabaud et al. 2015). Following the most plausible interpretation, the rocks crystallized from hybrid magmas (Holub 1997; Gerdes et al. 2000; Janoušek and Holub 2007). The rocks are ultrapotassic *sensu* Foley et al. (1987), feature high MgO and K₂O contents and elevated abundances of incompatible trace elements (Rb, Cs, Ba, U, Th). Relatively high Cr and Ni contents, accompanying elevated MgO, are considered a signature of melt derived from mantle source. The other component in the parental magma was a leucogranite melt of crustal derivation (Holub 1997; Janoušek and Holub 2007).

It will be shown that the presently studied phlogopite pyroxenite, localized in Bohemian Forest area (Moldanubian Zone) in Bohemian Massif [WGS84: N48°44'01.3", E14°00'28.3"], exhibits mineralogical and geochemical

similarities and genetic affinity to durbachites. Whereas in the published papers on durbachites discussion of melt origins and magma mixing prevailed, the newly obtained data on phlogopite pyroxenite indicate a role of fractional crystallization in evolution of durbachitic magmas. Breiter (2008) and Parat et al. (2010) also presented information supporting role of fractional crystallization in genesis of durbachites of the Třebíč Pluton, western Moravia, Czech Republic.

The existence of relatively abundant fine-grained enclaves in durbachites, having a more mafic composition (Holub 1997), amphibole–phlogopite ultramafic rocks and amphibole–phlogopite quartz diorites intruded mainly in the Prachatice Granulite Massif (Hejtman 1975; Breiter and Koller 2009) represent additional reasons to discuss possible role of fractional crystallization in evolution of durbachitic magmas. We will show that comparison of new data on phlogopite pyroxenite with published ones on durbachitic rocks presents evidence that both the processes were important in generation of the phlogopite pyroxenite.

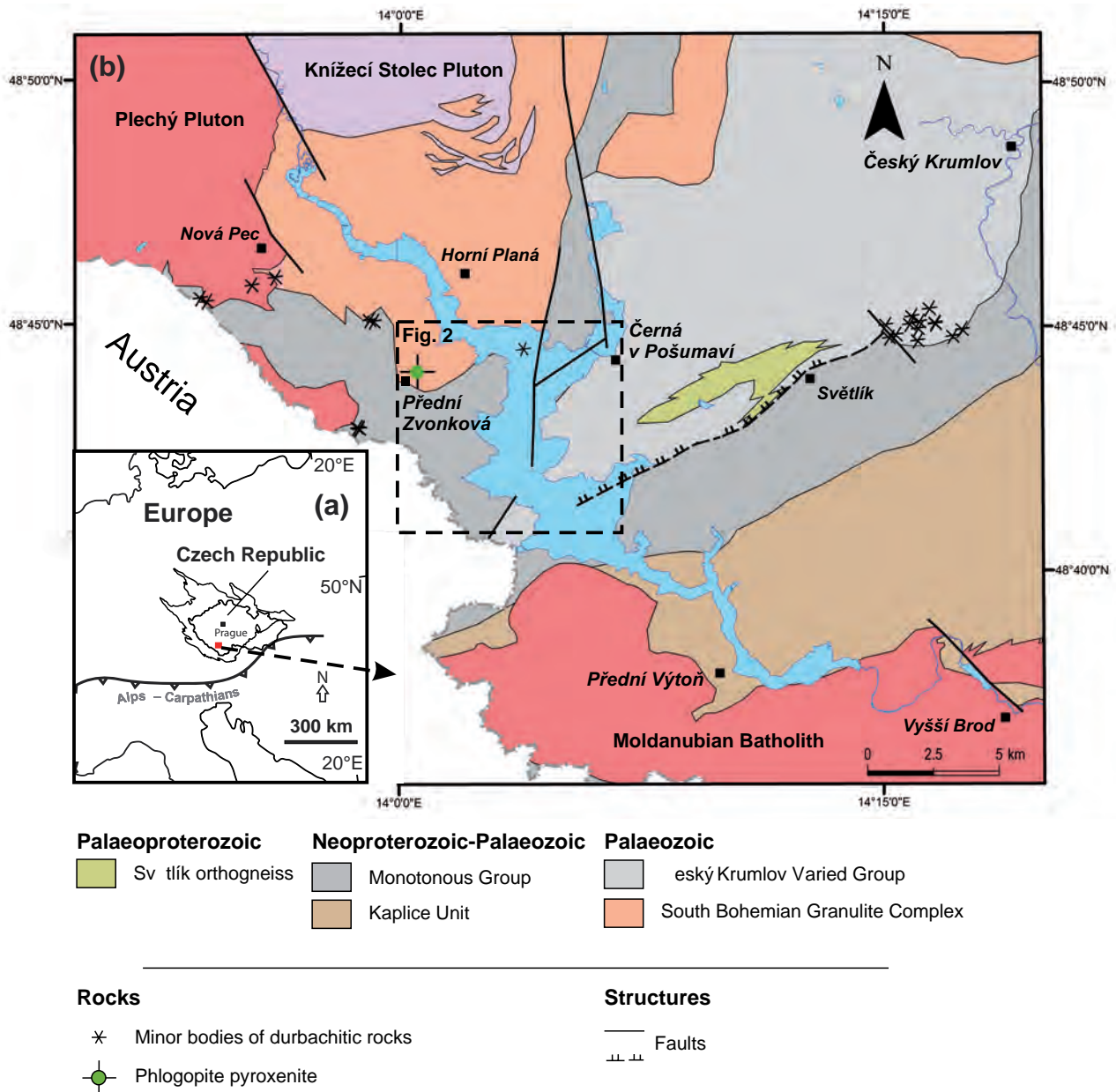


Fig. 1a – The simplified sketch of Europe with outline of the Bohemian Massif, marked position of the Czech Republic and the basement outcrop area. **b** – Geological sketch of the Šumava/Bohemian Forest (Böhmerwald) area (Moldanubian Zone) (adopted and modified after the geologic map 1 : 50 000, sheets Nová Pec 32–14, Český Krumlov 32–23, and Vyšší Brod 32–41).

As an interesting aspect of intrusion mechanisms appear incomparable dimensions of intrusions/plutons of various members of the durbachitic group. Whereas amphibole–biotite quartz syenite and quartz monzonite to melagranite constitute the large Knížecí Stolec Pluton (Fig. 1b; Verner et al. 2008), ultramafic to mafic amphibole–phlogopite intrusions in the Prachatice Granulite Massif attain usually dimensions only of tens to hundred metres (Hejtman 1975). The studied phlogopite pyroxenite from Přední Zvonková, indicated by geophysical data as a plug or lens 1 km in diameter, comes near to the small-size category of mafic rocks in the Prachatice

Granulite Massif. The present discovery of durbachitic phlogopite pyroxenite represents the rare rock-type in the Moldanubian Zone of the Bohemian Massif.

2. Geological setting

2.1. Moldanubian Zone of the Bohemian Massif

The study area is located in the Moldanubian Zone of the Bohemian Massif (Fig. 1a) in the Šumava/Bohemian

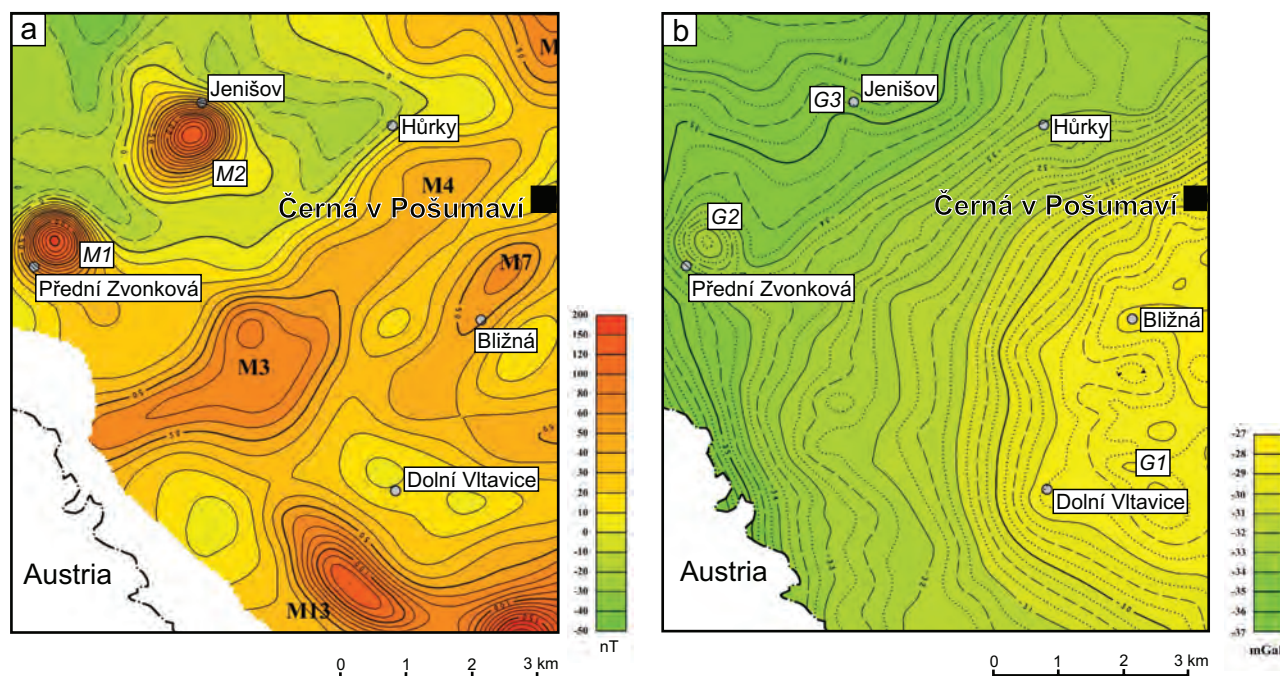


Fig. 2a – Airborne magnetic map with M1 anomaly near village of Přední Zvonková at the western margin of the area; M2 anomaly 2 km to the NE probably indicates similar rocks but the body is under water; **b** – Gravity map showing G2 and G3 anomalies coinciding with location of M1 and M2 anomalies. Data from Šrámek (2010).

Forest (Böhmerwald) region (Fig. 1b) and close to the Bavaricum domain. The Moldanubian Zone is interpreted as a root zone of the Variscan belt, resulting from collision of Gondwana with Laurasia (e.g., Schulmann et al. 2009). Metamorphic rocks of the Moldanubian Zone include mainly amphibolite-facies gneisses and migmatites with early Palaeozoic and late Proterozoic protolith ages (Košler et al. 2013), as well as high-pressure granulites, often with lenses or larger bodies of garnet and spinel peridotites and eclogites (Vrána et al. 1995). Subdivision of the Moldanubian Zone was presented in Dallmeyer et al. (1995) and McCann (2008); stratigraphy and lithology were characterized by Fiala et al. (1995). Important is the presence of several Variscan granitoid plutonic complexes including many scattered occurrences of ultrapotassic amphibole–biotite granitoid rocks (durbachites) (Holub 1997; Janoušek and Holub 2007; Žák et al. 2014).

2.2. Field data

Phlogopite pyroxenite body has been found by field assessment of a striking gravimetric and magnetometric anomaly, circular in plan and 1 km in diameter, near the village of Přední Zvonková, Český Krumlov region, southern Bohemia (Figs 1b, 2a–b). This work was conducted in course of compilation of the geologic map 1 : 25 000, sheet Černá v Pošumaví (Vrána et al. 2010).

Phlogopite pyroxenite occurs near contact of migmatites of the Monotonous Unit with retrogressed felsic granulites of the southern margin of the Křišťanov Granulite Massif (Fig. 1). This place is located 8 km south of the Knížecí Stolec durbachite pluton, 90 km² in area (Verner et al. 2008).

Airborne magnetometry survey (Šalanský and Manová 1988; Šrámek 2010) identified two small prominent anomalies, marked M1 and M2 (Fig. 2a). The anomaly M1 coincides with the body of phlogopite pyroxenite, as confirmed by fieldwork. The anomaly M2 is probably caused by a similar rock as M1; however, the region is flooded by the Lipno dam lake.

Gravimetry of wide area is based on detailed survey, including four stations per 1 km² (Vrána and Šrámek 1999). Anomalies G2 and G3 (Fig. 2b) coincide with the magnetometry anomalies M1 and M2. The gravity effect is caused by phlogopite pyroxenite with measured density of 3.1 g.cm⁻³, sampled in the area of the G2/M1 anomaly. Phlogopite pyroxenite shows a strong contrast against the local country rocks – migmatite, felsic granulite and paragneiss (with densities of 2.65–2.70 g.cm⁻³; Šrámek 2010). The gravimetry information indicates that the subsurface vertical dimensions do not exceed 100 m. Thus a lens-shaped circular body or a tectonic segment of a former plug would fit the gravimetry data.

3. Methods

3.1. Electron microprobe analysis

Analyses of the major rock-forming and selected accessory minerals were done with fully automated CAMECA SX-100 electron microprobe, employing $\Phi(\rho z)$ correction procedure (Pouchou and Pichoir 1985) at Joint Laboratory of Electron Microscopy and Microanalysis, Department of Geological Sciences, Masaryk University, and Czech Geological Survey, Brno, Czech Republic (P. Gadas). Analyses of clinopyroxene, orthopyroxene, and amphibole were performed typically at an acceleration voltage of 15 kV, currents of 20–40 nA and spot size of 5–10 μm . For phlogopite, chlorite and plagioclase, the beam current was 10–15 nA and spot size 2 μm . For sulphides beam current 20 nA with 25 kV acceleration voltage and 1 μm beam diameter were used. Minor-element interferences have been checked routinely and corrected for by measuring the corresponding standards. Calculation of mineral analyses to apfu was done using the spreadsheets by Tindle (2015).

3.2. Whole-rock geochemical analyses

Samples (*c.* 15–30 kg) were crushed in the laboratories of the Czech Geological Survey Prague–Barrandov (CGS) to grain fraction 2–4 cm by steel jaw crusher, homogenized and split to 500–1500 g. Finally, aliquots of *c.* 300 g were grinded in an agate mill. Selected major-element analyses were carried out by wet chemistry at CGS (Dempírová 2010). The relative 2σ uncertainties were better than 1 % (SiO_2), 2 % (FeO), 5 % (Al_2O_3 , K_2O , Na_2O), 7 % (TiO_2 , MnO, CaO), 6 % (MgO) and 10 % (Fe_2O_3 , P_2O_5).

Total abundances of the several minor elements were analysed in the Acme Analytical Laboratories (Vancouver) Ltd., Canada by ICP-OES following a lithium metaborate or tetraborate fusion and dilute nitric digestion of a 0.2 g sample (**method 4A**). The REE and refractory metals were determined by ICP-MS following a lithium metaborate or tetraborate fusion and nitric acid digestion of a 0.2 g sample (**method 4B**). In addition, separate 0.5 g splits were dissolved in aqua regia and analysed by ICP-MS to report the precious and base metals (**method 1DX**). For further analytical details, see <http://acmelab.com>.

Interpretation and plotting of the whole-rock geochemical data was facilitated by the freeware R-language package *GCDkit*, version 3.0 beta (Janoušek et al. 2006, 2011).

3.3. Sr–Nd isotopes

For the radiogenic isotope determinations, samples were dissolved using a combined HF–HCl–HNO₃ digestion.

Strontium and bulk REE were isolated from the matrix following the exchange chromatography techniques of Pin et al. (1994), i.e. using PP columns filled with Sr.spec and TRU.spec Eichrom resins, respectively. The Nd was further separated from the REE fraction on PP columns with Ln.spec Eichrom resin (Pin and Zalduegui 1997). Further analytical details were reported by Míková and Denková (2007).

Isotopic analyses of Sr were performed on a Finnigan MAT 262 thermal ionization mass spectrometer (TIMS) housed at the CGS in dynamic mode using a single Ta filament. Isotopic ratios of ¹⁴³Nd/¹⁴⁴Nd were acquired on MC ICP-MS Finnigan Neptune at Czech Geological Survey. The ¹⁴³Nd/¹⁴⁴Nd ratios were corrected for mass fractionation to ¹⁴⁶Nd/¹⁴⁴Nd = 0.7219 (Wasserburg et al. 1981), ⁸⁷Sr/⁸⁶Sr ratios assuming ⁸⁶Sr/⁸⁸Sr = 0.1194. External reproducibility is estimated from repeat analyses of the JNd11 [Tanaka et al. 2000; ¹⁴³Nd/¹⁴⁴Nd = 0.512101 ± 14, (2σ , $n = 10$) and NBS 987 [⁸⁷Sr/⁸⁶Sr = 0.710247 ± 26, (2σ , $n = 22$)] isotopic standards. The decay constants applied to age-correct the isotopic ratios are from Steiger and Jäger (1977 – Sr) and Lugmair and Marti 1978 – Nd). The ϵ_{Nd} values were obtained using Bulk Earth parameters of Jacobsen and Wasserburg (1980), the single-stage Depleted Mantle Nd model ages ($T_{\text{DM}}^{\text{Nd}}$) were calculated after Liew and Hofmann (1988).

3.4. Re–Os geochemistry

Rhenium and osmium separation was performed at the Institute of Geology AS CR, v.v.i. The powders (~ 2 g) were mixed with ¹⁸⁵Re and ¹⁹⁰Os spikes and dissolved using *High Pressure Asher (Anton Paar)* apparatus with ~4 ml of concentrated HCl and ~5 ml of concentrated HNO₃ at 320 °C and 120 bar for 12 hours. After digestion, osmium was separated using solvent extraction to CCl₄ and back reduction to HBr (Cohen and Waters 1996). The final fraction was purified by microdistillation (Birck et al. 1997). Rhenium was separated by anion exchange chromatography using AG 1×8 resin (BioRad). The samples were loaded into columns in chloride form (1M HCl) and Re fraction was collected by 6M HNO₃.

Rhenium concentrations were determined on sector field single-collector ICP-MS Element 2 (Thermo) coupled with desolvation nebulizer Aridus II at the Institute of Geology CAS, v.v.i. The isotopic fractionation was corrected using a linear law and different 300 ppt Re standard solution (NIST 3143, E-Pond). Osmium isotopic compositions were analysed as OsO₃⁻ using a Finnigan MAT 262 TIMS with modifications for measuring negative ions (N-TIMS) at the CGS. All samples were measured using an electron multiplier in a peak-jumping mode. The samples were loaded onto Pt filaments and dried. The Ba(OH)₂ activator was subsequently added



Fig. 3 Texture of phlogopite pyroxenite. Note numerous light grey to moderate grey euhedral sections of pyroxene up to 5 mm long. Light beige grains are phlogopite crystals split parallel to the basal cleavage. Sulphide aggregates up to 5 mm across show a pepper-and-salt pattern.

for electron production. The measured Os isotopic ratios were corrected offline for oxygen and osmium mass fractionation using $^{192}\text{Os}/^{188}\text{Os} = 3.08271$ (Shirey and Walker 1998). Osmium concentrations were obtained using isotope dilution technique. After that, offline $^{187}\text{Os}/^{188}\text{Os}$ correction for blank and spike contribution was applied. External precision for the 300 pg Os UMCP standard solution (Johnson–Matthey Co.) was 0.2 % (2σ). The γOs parameter represents percent deviation from Primitive Mantle with a $^{187}\text{Os}/^{188}\text{Os}$ value of 0.1296 (Meisel et al. 2001). Osmium model ages (T_{MA}) were calculated using Primitive Mantle $^{187}\text{Re}/^{188}\text{Os}$ and $^{187}\text{Os}/^{188}\text{Os}$ values of Meisel et al. (2001) and decay constant of Smoliar et al. (1996).

Tab. 1 Estimates of modal composition of phlogopite pyroxenites (vol. %)

Sample	SV235A	SV235B	SV235C
clinopyroxene	23	14	35
orthopyroxene	25	—*	—*
Amp primary	6	32	25
Amp second.	6	32	23
phlogopite	27	9	7
chlorite	—	4	—
plagioclase	3	—	2
quartz	—	—	2
apatite	6.7	7.0	3.7
sulphides	3	2.1	2.3
titanite	—	+	+
carbonate	—	—	+
graphite	+	+	+

—* orthopyroxene replaced by actinolite and anthophyllite

4. Results

4.1. Magnetometry and gravimetry

Given the flat relief in the area and soil cover, geophysical data (magnetometry and gravimetry) provide informa-

tion on probable shape and dimensions of the pyroxenite body. The site corresponds to the centre of the geophysical anomalies M1 and G2 (Fig. 2). Several blocks of phlogopite pyroxenites (Fig. 3) up to 70 cm long were located at a stone heap, which resulted from clearing the local pasture. Three of the blocks were sampled for chemical analyses: 235A, 235B, 235C.

4.2. Petrography and mineral chemistry

The medium-grained rock, sample A, contains 27 vol. % phlogopite, 23 % diopsidic clinopyroxene, 25 % orthopyroxene, abundant apatite (c. 7 %), as well as minor plagioclase (3 %) and pyrrhotite (3 %) (Tab. 1). Volume % estimates for apatite and pyrrhotite are supported by S and P_2O_5 contents in chemical analyses. Owing to late postmagmatic reactions, orthopyroxene is locally replaced by fibrous aggregates of actinolite and anthophyllite. A part of the sample shows numerous subhedral to euhedral pyroxene crystals (Figs 3–4) as would be expected in a cumulate rock. Samples B and C show effects of a more or less intense replacement of pyroxenes by a light brown tremolitic amphibole and of orthopyroxene by tremolite + anthophyllite aggregates. The sample C was significantly enriched in diopside (Tab. 1) with clear tendency to concentrate in Cpx-rich bands.

Colourless diopside is highly magnesian with $mg\# = 0.80\text{--}0.81$ ($mg\# = \text{Mg}/(\text{Mg} + \text{Fe})$). It contains low Al, Cr and Na (Tab. 2). Orthopyroxene is widely preserved in sample A (Fig. 4a–c). It has $mg\# = 0.72$ and contains low Al, Cr and Ca. Reddish-brown phlogopite is also highly magnesian with $mg\# = 0.78$, 3.9–4.0 wt. % TiO_2 , 0.39–0.43 wt. % Cr_2O_3 and 0.45–0.46 wt. % BaO. There is a light brownish to ochre amphibole (Fig. 4d), with textural relations indicating a late primary magmatic crystallization, in part via orthopyroxene replacement. It has $mg\# = 0.89\text{--}0.92$ and contains 4.3 wt. % Al_2O_3 . It is classified as magnesiohornblende compositionally close

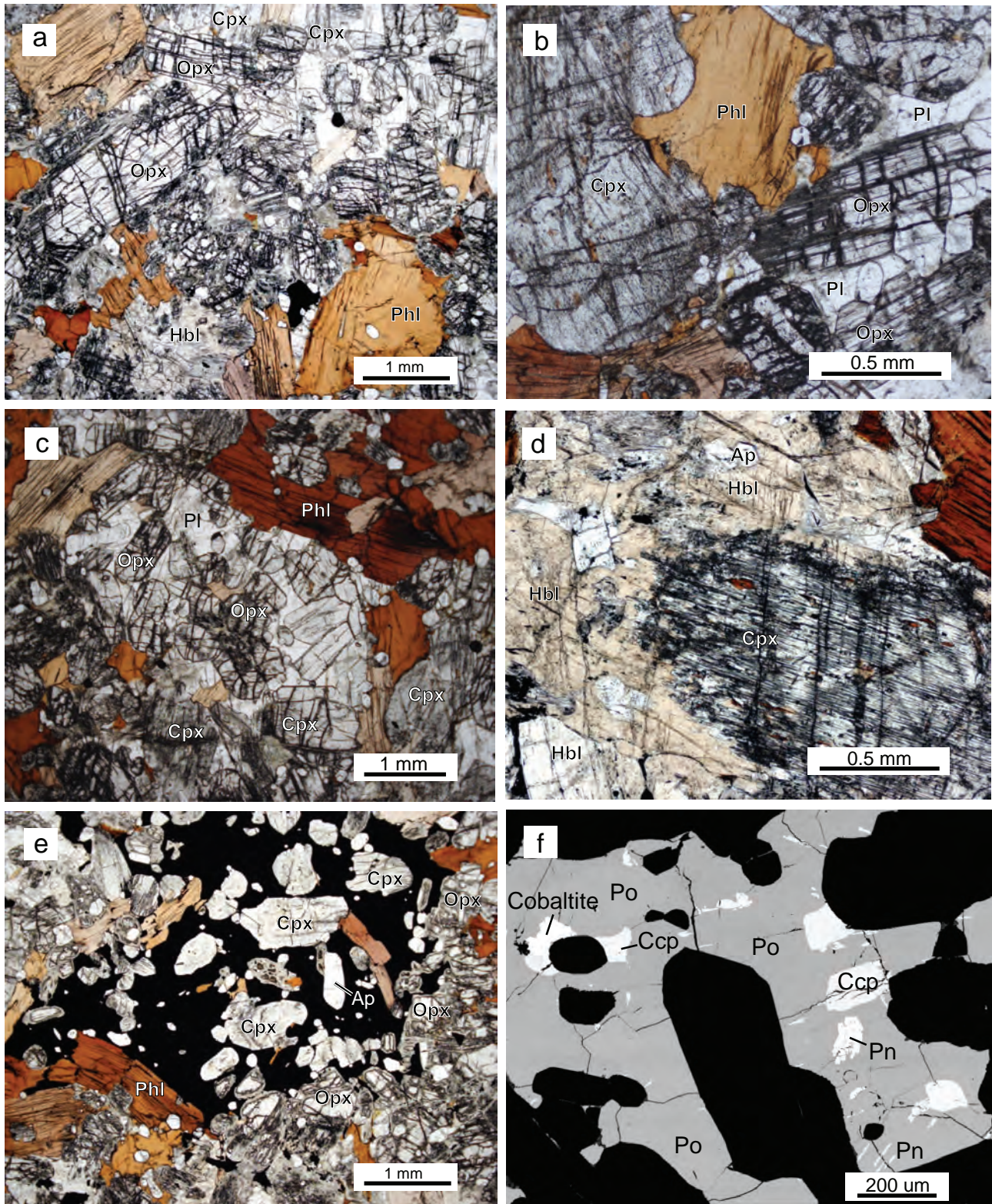


Fig. 4a – Aggregate of subhedral orthopyroxene crystals in contact with deformed phlogopite, apatite and minor interstitial plagioclase; **b** – Subhedral orthopyroxene, clinopyroxene and minor interstitial plagioclase; **c** – Poikilitic phlogopite carrying pyroxene inclusions and bordering pyroxene aggregate; **d** – Light brown primary amphibole replacing a large Opx crystal; **e** – Sulphide aggregate with inclusions of pyroxene, phlogopite and apatite; **f** – Poikilitic aggregate of pyrrhotite (Po) with unmixed pentlandite (Pn), chalcopyrite (Ccp) and cobaltite. Transmitted plane-polarized light photomicrographs (a–e) and Back-scattered electron (BSE) image (f). All mineral abbreviations are after Whitney and Evans (2010).

Tab. 2 Electron-microprobe analyses of silicate minerals (wt. % and apfu)

analysis No	Orthopyroxene		Clinopyroxene		Amphibole	Phlogopite		Plagioclase		Anthophyllite	Actinolite	Apatite	
	3	2	6	8	13 [†]	9	10	14	16	26 [†]	27 [†]	11	18
SiO ₂	54.96	55.06	53.86	53.83	53.76	39.26	38.97	58.61	58.26	56.45	57.15	0.15	0.14
TiO ₂	0.30	0.19	0.17	0.22	0.63	3.94	4.01			0.06	0.09		
Al ₂ O ₃	0.69	0.67	0.90	1.21	4.26	14.21	13.96	25.90	26.46	0.48	0.65		
Cr ₂ O ₃	0.06	0.05	0.23	0.17	0.17	0.43	0.39			0.04	0.05		
V ₂ O ₃	0.00	0.04	0.09	0.04	0.13	1.19	1.26			0.00	0.01		
Fe ₂ O ₃ [‡]					2.78								
FeO					4.28							0.13	0.00
FeOt	17.58	17.75	7.76	7.79		9.41	9.45	0.03	0.05	18.14	10.80		
MnO	0.35	0.37	0.26	0.24	0.11	0.03	0.03			0.63	0.44	0.06	0.03
MgO	25.37	25.45	16.99	16.56	19.02	19.12	18.62			20.80	20.25	0.04	0.00
CaO	1.30	1.43	20.17	20.49	12.23	0.00	0.01	8.10	8.77	1.04	8.43	54.88	55.45
SrO								0.23	0.22			0.11	0.11
PbO												0.03	0.00
Na ₂ O	0.05	0.05	0.24	0.28	0.76	0.29	0.27	6.90	6.67	0.10	0.21	0.09	0.05
K ₂ O	0.00	0.00	0.02	0.00	0.37	9.30	9.44	0.28	0.26	0.00	0.03		
BaO						0.46	0.45						
P ₂ O ₅												41.07	40.40
ZnO	0.00	0.07	0.00	0.07	0.00	0.04	0.00			0.00	0.00		
NiO	0.00	0.01	0.00	0.00	0.01	0.03	0.02			0.02	0.00		
F					0.38	0.28	0.29			0.05	0.10	2.84	2.21
Cl						0.03	0.02					0.13	0.15
La ₂ O ₃												0.08	0.05
Ce ₂ O ₃												0.16	0.16
Pr ₂ O ₃												0.06	0.05
Nd ₂ O ₃												0.15	0.07
SO ₃												0.01	0.00
H ₂ O [‡]					1.97	4.03	3.98			2.08		0.40	0.67
O=F,Cl					-0.16	-0.12	-0.13			-0.02	-0.04	-1.22	-0.96
Total	100.67	101.17	100.78	101.01	100.74	101.97	101.04	100.10	100.69	99.93	98.20	99.57	98.61
Number of ions													
Si	1.988	1.986	1.974	1.970	7.473	5.648	5.667	2.627	0.597	8.025	7.990	0.013	0.012
Al ^{IV}	0.012	0.014	0.026	0.030	0.527	2.352	2.333	1.368	1.391	0.000	0.010		
Al ^{VI}	0.017	0.015	0.013	0.022	0.171	0.058	0.060			0.080	0.097		
Ti	0.008	0.005	0.005	0.006	0.066	0.426	0.439			0.006	0.009		
Cr	0.002	0.001	0.007	0.005	0.019	0.049	0.045			0.004	0.006		
Fe ³⁺					0.291								
Fe ²⁺	0.532	0.535	0.222	0.226	0.497	1.132	1.149	0.001	0.002	2.155	1.263	0.009	0.000
Mn	0.011	0.011	0.008	0.007	0.013	0.004	0.004			0.076	0.052	0.004	0.002
Mg	1.367	1.368	0.928	0.903	3.942	4.100	4.036			4.405	4.221	0.005	0.000
Ca	0.050	0.055	0.792	0.803	1.822			0.388	0.419	0.158	1.263	4.999	5.102
Sr												0.006	0.006
Pb												0.001	0.000
Zn					0.000	0.004	0.000			0.000	0.000		
Ni	0.000	0.000	0.000	0.000	0.001	0.003	0.002			0.000	0.002		
Na	0.004	0.003	0.017	0.020	0.205	0.081	0.076	0.599	0.576	0.028	0.057	0.015	0.008
K	0.000	0.000	0.001	0.001	0.066	1.707	1.751	0.016	0.015	0.000	0.005		
Ba					0.000	0.026	0.026			0.001	0.001		
P												2.964	2.938
F					0.167	0.127	0.133			0.022	0.044	0.766	0.600
Cl					0.002	0.007	0.005			0.002	0.005	0.019	0.022
La												0.002	0.002
Ce												0.005	0.005
Pr												0.002	0.002
Nd												0.005	0.002
S												0.001	0.000
OH [‡]					1.831	3.865	3.862			1.975	1.951	0.215	0.378
Total	3.990	3.995	4.008	4.006	17.092	19.590	19.589	5.000	5.000	16.940	16.975	9.031	9.079
Mg/(Mg+Fe)	0.720	0.719	0.807	0.800	0.888	0.784	0.778			0.672	0.770		

[†] 13 – primary magnesianhornblende close to tremolite; 26 – secondary anthophyllite; 27 – secondary actinolite in mixture with anthophyllite

[‡] H₂O content calculated from stoichiometry as is also ferrous/ferric ratio in primary amphibole

Tab. 3 Electron-microprobe analyses of sulphides

Analysis No.	3	9	10	2
mineral	pyrrhotite	chalcopyrite	cobaltite	sphalerite
S	38.35	34.81	19.43	33.13
As	0.04	0.00	45.02	0.02
Fe	58.86	29.96	5.30	10.33
Co	0.00	0.00	23.60	0.13
Ni	0.33	0.03	6.85	0.01
Cu	0.00	34.54	0.00	1.31
Zn	0.00	0.02	0.01	54.02
Total	97.58	99.34	100.21	98.95
No. of atoms				
S	1.062	2.005	1.000	1.000
As	0.000	0.000	0.991	0.000
Fe	0.935	0.991	0.157	0.178
Co	0.000	0.000	0.660	0.002
Ni	0.003	0.000	0.192	0.000
Cu	0.000	1.004	0.000	0.020
Zn	0.000	0.000	0.000	0.800
Total	2.000	4.000	3.000	2.000

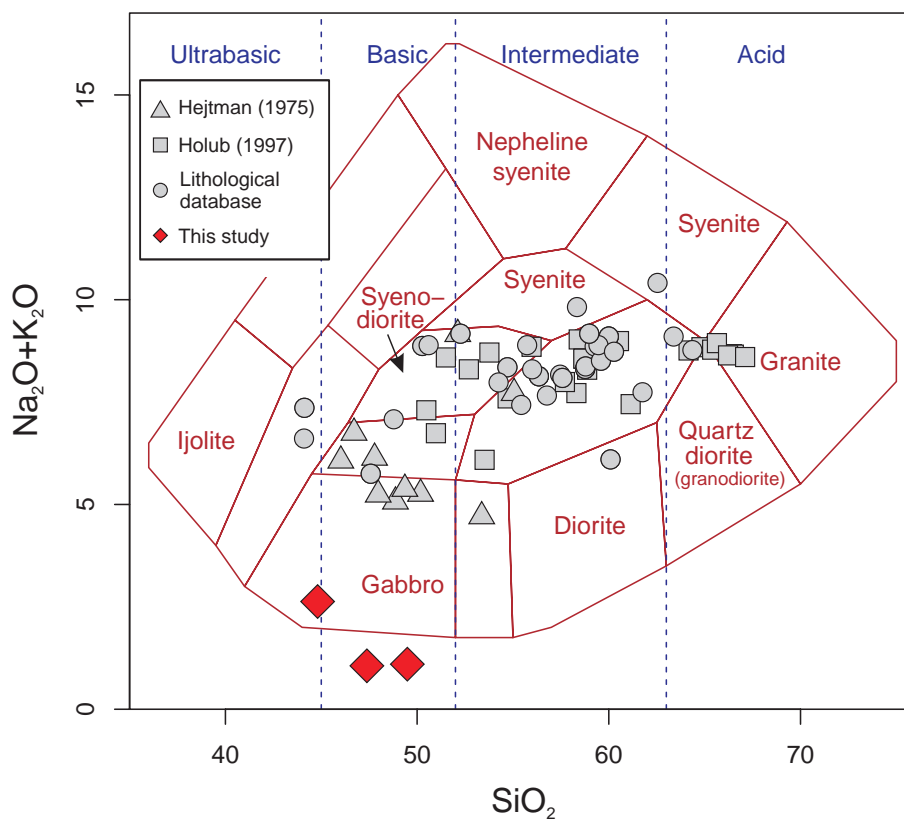
to the tremolite–actinolite–magnesianhornblende triple point (Leake et al. 2003).

Accessory plagioclase is intermediate andesine ($An_{0.39-0.42}Ab_{0.58-0.60}Or_{0.01}$) with 0.22–0.23 wt. % SrO. Fluorapatite (Tab. 2) is a relatively important phase making 3.7–7.0 vol. % of all samples. It contains 2.2–2.8 wt. % F, but relatively low light REE and Sr contents.

Tab. 4a Chemical composition of phlogopite pyroxenites from Přední Zvonková (major and minor components; wt. %)

Sample	SV235A	SV235B	SV235C
SiO ₂	44.81	47.38	49.49
TiO ₂	1.02	0.44	0.47
Al ₂ O ₃	5.36	3.62	3.12
Fe ₂ O ₃	1.33	2.26	2.73
FeO	10.70	9.63	7.47
MgO	17.35	18.81	15.15
MnO	0.190	0.233	0.223
CaO	9.51	9.84	14.71
SrO	0.018	0.017	0.015
BaO	0.123	0.020	0.025
Li ₂ O	0.004	0.003	0.004
Na ₂ O	0.33	0.20	0.45
K ₂ O	2.30	0.86	0.65
P ₂ O ₅	2.759	2.489	1.526
F	0.358	0.196	0.134
CO ₂	0.23	0.10	0.65
C	0.067	0.098	0.157
S	1.140	0.852	0.932
H ₂ O ⁺	2.12	2.80	1.87
H ₂ O ⁻	0.16	0.09	0.12
F-eq.	-0.151	-0.083	-0.056
S-eq.	-0.285	-0.213	-0.233
Sum	99.87	99.94	99.89
FeO _t	11.90	11.66	9.93
mg#	78.75	80.52	80.90

mg# = 100*Mg/(Mg + Fe) with total Fe, atomic values



It is notable that the rocks are free of magnetite and an oxidic Cr-rich phase. Phlogopite containing 0.39–0.43 wt. % Cr₂O₃ is the main carrier of chromium, being followed by diopside. Minor accessory titanite, graphite and allanite were also detected.

Sulphide aggregates occur in all three samples. They are typically 1 to 3 mm long in samples A and B and 1 mm or smaller in sample C. The aggregates apparently evolved via crystallization on silicate interfaces, gradual coarsening and coalescence to 3 mm aggregates carrying numerous inclusions of pyroxenes, phlogopite and apatite, making

Fig. 5 The total alkalis versus silica (TAS) diagram modified by Cox et al. (1979) for the phlogopite pyroxenites from Přední Zvonková, hornblende biotitites (Hejtman 1975), durbachites (Holub 1997) and durbachites (lithological database, Gürtlerová et al. 1997).

Tab. 4b Chemical composition of phlogopite pyroxenites from Přední Zvonková (trace elements excluding REE; ppm except for Au)

Sample	SV235A	SV235B	SV235C
Cr	*1420	2186.6	2299.1
Hf	1.8	3.3	2.9
Nb	7.7	10.2	7.7
Pb	3.2	1.5	20.3
Rb	162	27.1	13.2
Se	1.1	< 0.5	< 0.5
Ta	0.5	8.4	5.7
Th	9.0	14.6	8.5
Au (ppb)	1.8	2.0	2.7
Cd	–	0.8	0.4
Cs	6.9	5.0	1.6
Cu	168.3	118.6	159.4
Ga	8.6	6.3	7.0
Ge	–	14.3	11.4
In	–	< 0.1	< 0.1
Ir	–	< 0.1	< 0.1
Mo	1.5	3.1	1.8
Nb	7.7	10.2	7.7
Ni	246.7	211.1	256.9
Sn	–	5	< 1
Ti	–	2558	2601
Tl	1.1	0.3	0.3
U	4.5	5.0	3.4
V	382	319.1	439.7
W	–	6.4	2.1
Zn	45	213	84
Zr	55.5	95.0	80.0
Sr	152.0	140.3	125.3
Sc	–	42.1	58.7
Ba	1105	178.9	220.1
Be	–	2.7	2.1
Co	100.7	73	76
Ag	0.1	< 0.8	< 0.8
Cd	–	< 0.8	< 0.8
Cs	–	< 10	< 10
Laboratory	1, 2	2	2

Laboratories and methods: 1 – Czech Geological Survey, Prague, *XRF; 2 – Acme Laboratories Ltd., Vancouver, Canada, combination of methods, ICP-MS (*in italic*)

30 to 50 % by volume of the sulphide aggregate. The aggregates contain (by estimate) 90 vol. % pyrrhotite, 6 % chalcopyrite, 1–2 % cobaltite and 2–3 % pentlandite as a flame-shaped unmixed phase in pyrrhotite. Composition of sulphides is presented in Tab. 3. Several mm long aggregates of pyrrhotite enclose individual grains of pyroxenes, phlogopite and apatite, and indicate tendency to local segregation of sulphides (Fig. 4e–f).

4.3. Whole-rock geochemistry

Dataset of the whole-rock major- and trace-element analyses of phlogopite pyroxenites contains three samples (see

Fig. 1b for position of the sampled locality). For comparison, published whole-rock analyses of major- and trace-elements of durbachitic rocks are used (Hejtman 1975; Holub 1997 and lithological database of Gürtlerová et al. 1997).

The studied samples are basic ($\text{SiO}_2 = 44.8\text{--}49.4$ wt. %). In the total alkalis versus silica (TAS) diagram, modified by Cox et al. (1979), the phlogopite pyroxenites occupy the gabbro field (Fig. 5). According to the mineral contents, the sample 235A is classified as a phlogopite websterite (Le Maitre ed. 2002). The samples B and C are difficult to classify with regard to strong alteration. The binary diagram mg\# [i.e. molar ratio $100 \times \text{MgO}/(\text{MgO} + \text{FeO})$] vs. MgO shows values corrected for the pyrrhotite enrichment in three phlogopite pyroxenites and literature data (Hejtman 1975; Holub 1997; Gürtlerová et al. 1997) (Fig. 6). The diagram underlines the highly magnesian character of phlogopite pyroxenites. The correlation of the mg\# values vs. major- and minor elements in the samples SV235A, B, C and literature data are presented in Fig. 7. It demonstrates the low contents of SiO_2 , Al_2O_3 , Na_2O and K_2O and high FeO , CaO and P_2O_5 of the pyroxenites relative to the common durbachitic rocks.

If compared with the lower continental crust (Taylor and McLennan 1995; Fig. 8a), the samples are enriched in Large-Ion Lithophile Elements (LILE; Cs, Rb, Th, U and K) and LREE. For Sr, Ti and HREE, the normalized values are close to one. The patterns also show troughs in High Field Strength Elements (HFSE; Ti, Zr, Hf). The

Tab. 4c Chemical composition of phlogopite pyroxenites from Přední Zvonková (rare earth elements; ppm)

Sample	SV235A	SV235B	SV235C
Y	34.9	30.5	30.3
La	45.8	41.3	30.7
Ce	132.1	99.5	76.3
Pr	18.37	11.56	8.85
Nd	89.3	82.9	62.8
Sm	19.83	18.92	15.22
Eu	2.31	2.16	1.81
Gd	13.87	12.50	10.52
Tb	1.67	1.45	1.34
Dy	7.50	6.82	6.61
Ho	1.26	1.12	1.13
Er	3.15	2.89	2.99
Tm	0.38	0.35	0.37
Yb	2.47	2.12	2.23
Lu	0.34	0.28	0.32
$(\text{La}/\text{Yb})_N$	12.5	13.18	9.29
$(\text{La}/\text{Sm})_N$	1.5	1.4	1.3
Eu/Eu*	0.43	0.43	0.44
ΣREE	338.4	284.0	221.2
Laboratory	2	1	1

$(\text{La}/\text{Yb})_N$ = elemental ratio of La and Yb normalized to average chondrite composition (Boynton 1984)

Eu/Eu* = europium anomaly calculated using the geometric mean of chondrite-normalized abundances of Sm and Gd

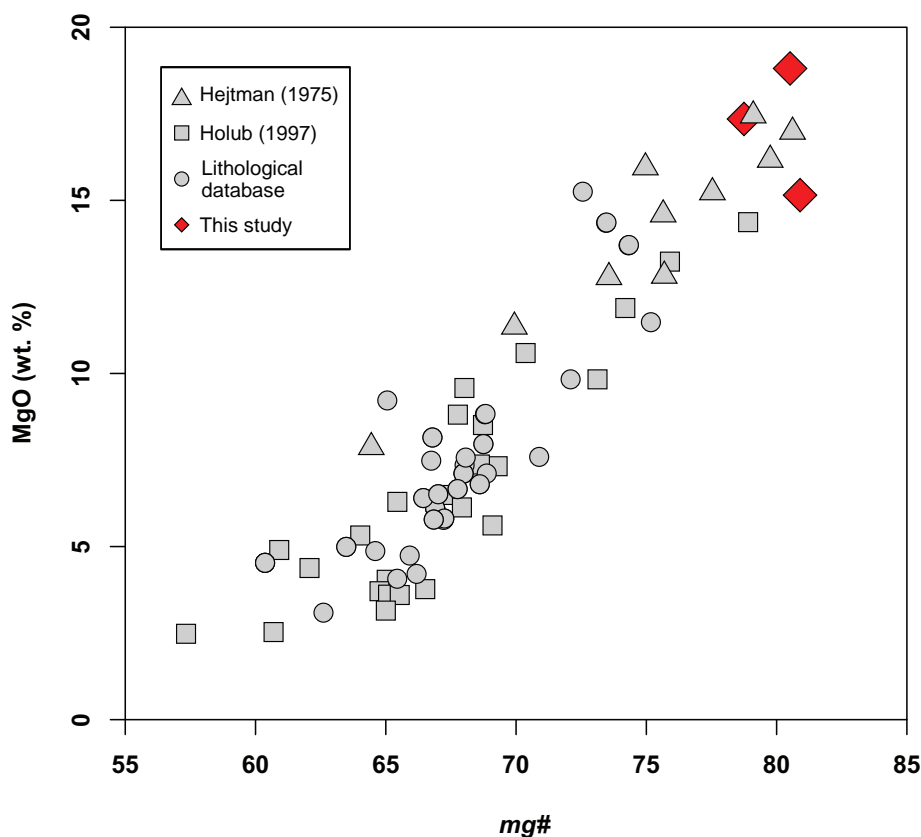


Fig. 6 Binary plot mg# vs. MgO (wt. %) with positive correlation. Phlogopite pyroxenite values are corrected for the pyrrhotite content.

REE contents vary moderately ($\Sigma\text{REE} = 221\text{--}338$). The chondrite-normalized patterns (Boynton 1984; Fig. 8b) are steep ($\text{La}_N/\text{Yb}_N = 9\text{--}13$). Typical is the flat course of the LREE segment ($\text{La}_N/\text{Sm}_N = 1.3\text{--}1.5$) and the presence of negative Eu anomalies ($\text{Eu}/\text{Eu}^* = 0.4$).

4.4. Radiogenic isotopes

4.4.1. Sr–Nd isotopic data

In order to further constrain geochemical variations, all three samples were analysed for their Sr–Nd isotopic composition (Tab. 5). The phlogopite pyroxenites are characterized by evolved crust-like Sr–Nd isotopic signatures ($^{87}\text{Sr}/^{86}\text{Sr}_{337} = 0.7093\text{--}0.7143$; $\epsilon_{\text{Nd}_{337}} = -5.4$ to -5.6 ; Fig. 9). The depleted-

mantle Nd model ages calculated after Liew and Hofmann (1988) are $\sim 1.7\text{--}1.9$ Ga for the single-stage model.

4.4.2. Re–Os isotopic data

Two whole-rock samples (SV235A and C) were analysed for their Re–Os concentrations and $^{187}\text{Os}/^{188}\text{Os}$ compositions (Tab. 6). They yield variable Re contents of 1.62 and 2.96 ppb, respectively, at nearly similar Os concentrations (0.076 and 0.070 ppb). These result in high $^{187}\text{Re}/^{188}\text{Os}$ ratios of 107 and 236, respectively. Consequently, both samples exhibit markedly radiogenic present-day $^{187}\text{Os}/^{188}\text{Os}$ compositions of 0.4622 and 1.3230 with γ_{Os} values of +257 and +921. Osmium model ages yield values of 0.2 and 0.3 Ga.

Tab. 5 Sr–Nd isotopic data for phlogopite pyroxenites

Sample	Rb (ppm)	Sr (ppm)	$^{87}\text{Rb}/^{86}\text{Sr}$	$^{87}\text{Sr}/^{86}\text{Sr}$	2 SE ($^{87}\text{Sr}/^{86}\text{Sr}$) ₃₃₇	Sm (ppm)	Nd (ppm)	$^{147}\text{Sm}/^{144}\text{Nd}$	$^{143}\text{Nd}/^{144}\text{Nd}$	2 SE ($^{143}\text{Nd}/^{144}\text{Nd}$) ₃₃₇	$\epsilon_{\text{Nd}_{337}}$	T_{DM}^{Nd} (Ga)		
SV235A	161.5	152.0	3.0801	0.72404	18	0.709260	19.83	89.3	0.1342	0.512225*	7	0.511929	-5.37	1.7
SV235B	27.1	140.3	0.5598	0.71595	11	0.713266	18.92	82.9	0.1379	0.512232*	5	0.511928	-5.39	1.7
SV235C	13.2	125.3	0.3044	0.71578	12	0.714318	15.22	62.8	0.1465	0.512241*	5	0.511918	-5.59	1.9

Isotopic ratios with subscript '337' were age-corrected to 337 Ma; decay constants are from Steiger and Jäger (1977 – Sr) and Lugmair and Marti (1978 – Nd).

The ϵ_{Nd} values were obtained using Bulk Earth parameters of Jacobsen and Wasserburg (1980).

The single-stage Nd model ages (T_{DM}^{Nd}) were calculated after Liew and Hofmann (1988).

*Isotopic ratios of $^{143}\text{Nd}/^{144}\text{Nd}$ were obtained on MC-ICP-MS.

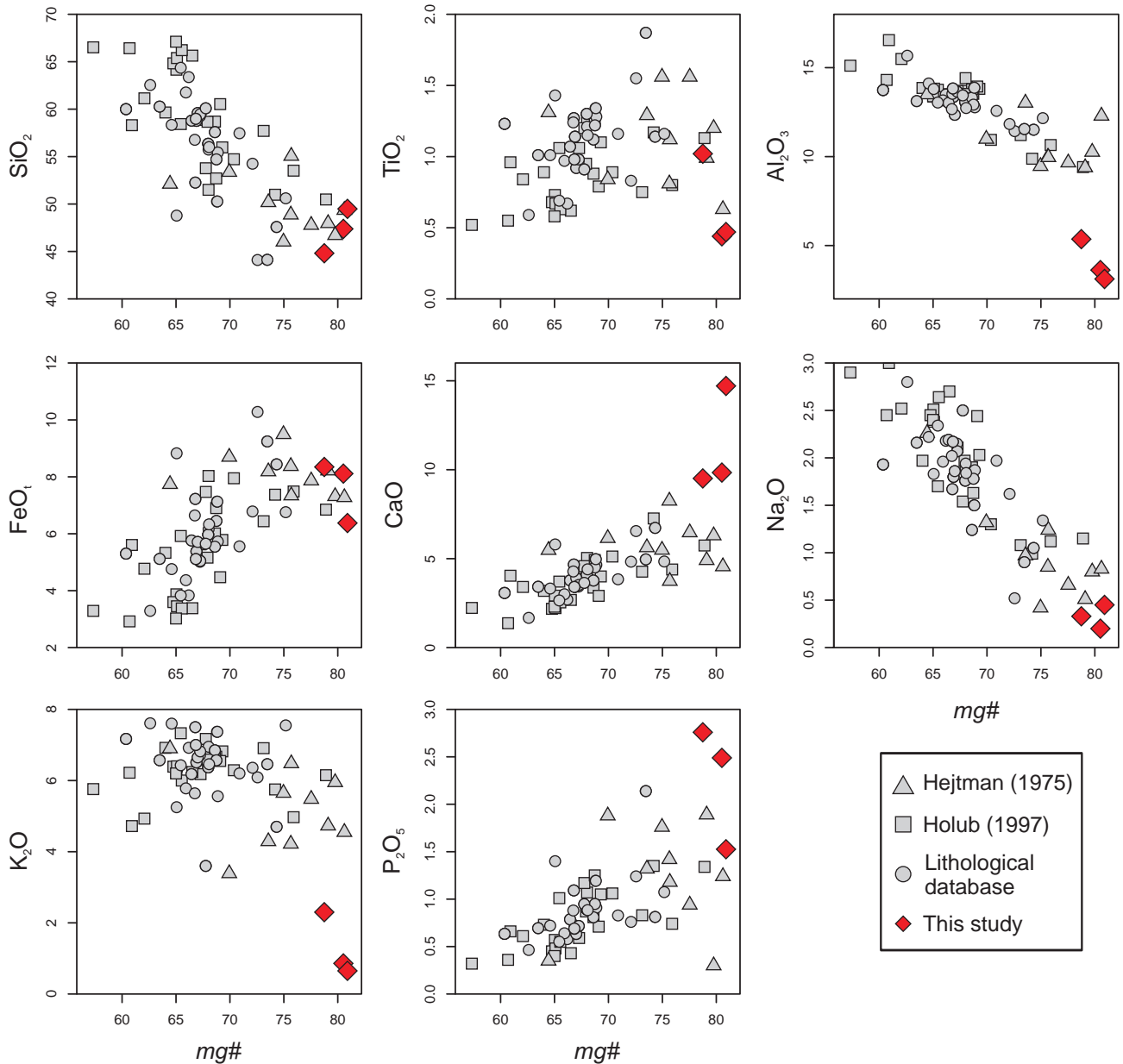


Fig. 7 Binary plots of mg# vs. major- and minor-element oxides (wt. %).

4.5. Geothermometry

Two-pyroxene thermometers of Bertrand and Mercier (1985), Brey and Köhler (1990) and Taylor (1998) gave temperatures of 969–1038 °C (Tab. 7). The Ca-in-orthopyroxene calculation following Brey and Köhler (1990) yielded somewhat lower average value of 917 °C. The coupled exchange of Ti and Fe²⁺ in biotite (Luhr et al. 1984) gave 1007 °C (Tab. 7). Geothermometry data were calculated always for two mineral pairs and the results in Tab. 7 are averages. Altogether these data indicate crystallization temperatures for phlogopite pyroxenite from Přední Zvonková in the range of ~970–1040 °C.

5. Discussion

5.1. Petrogenesis of the studied phlogopite pyroxenite

The studied phlogopite pyroxenites have ultramafic composition, and represent cumulates formed by fractional crystallization of a durbachitic melt. The euhedral/subhedral shape of pyroxenes, occurrence of diopside-enriched bands in sample SV235C, a strong enrichment in apatite and segregation of sulphides suggesting melt immiscibility, all accentuate the character

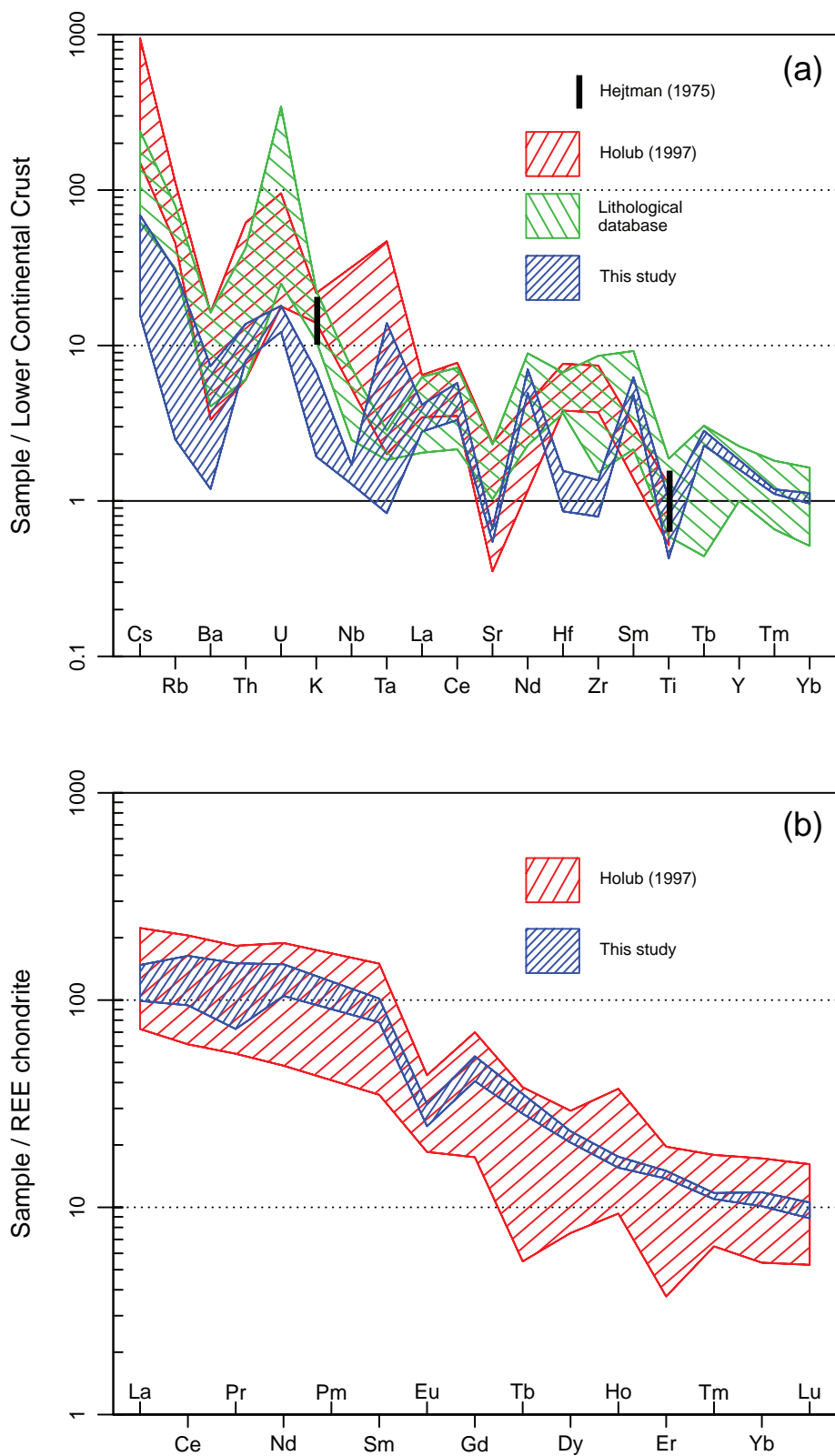


Fig. 8 Spider plots of (a) trace-element contents normalized by the average composition of the Lower Continental Crust (Taylor and McLennan 1995) and (b) REE abundances normalized by chondrite (Boynton 1984).

of the studied phlogopite pyroxenites as cumulates.

In the $mg\#$ vs. MgO plot (Fig. 6) amphibole–phlogopite rocks (Hejtman 1975) span a transitional array between durbachites, with lower $mg\#$ and MgO , and phlogopite pyroxenite cumulates. Binary diagrams of $mg\#$ values versus selected oxides, except TiO_2 , show linear relations for durbachitic rocks (Fig. 7). In most cases (Al_2O_3 , FeO , CaO , K_2O and P_2O_5) these are not followed by the studied phlogopite pyroxenites. Figure 10 underlines a notable enrichment in Cr and especially V in the studied pyroxenites probably due to preferential crystallochemical incorporation into the accumulated phlogopite.

Notable is the absence of zircon in phlogopite pyroxenites from Přední Zvonková. This indicates crystallization at temperatures higher than zircon saturation temperature, resulting in Zr retention in the residual melt.

The phlogopite pyroxenite geochemistry cannot be explained without incorporation of a granitic crustal component. Neodymium isotope geochemistry, as well as Re/Os relations, indicate a prolonged crustal residence of crustal material prior to its incorporation into the durbachitic melt. With regard to widespread replacement of pyroxenes by secondary amphiboles in samples B and C, the Sr isotopic composition was probably modified by activity of low-T fluids. Previous studies interpreted durbachitic rocks mainly as having crystallized from hybrid magmas developed via mixing of anomalous mantle-derived melts with crustal, leucogranitic magmas (Holub 1997; Janoušek and Holub 2007).

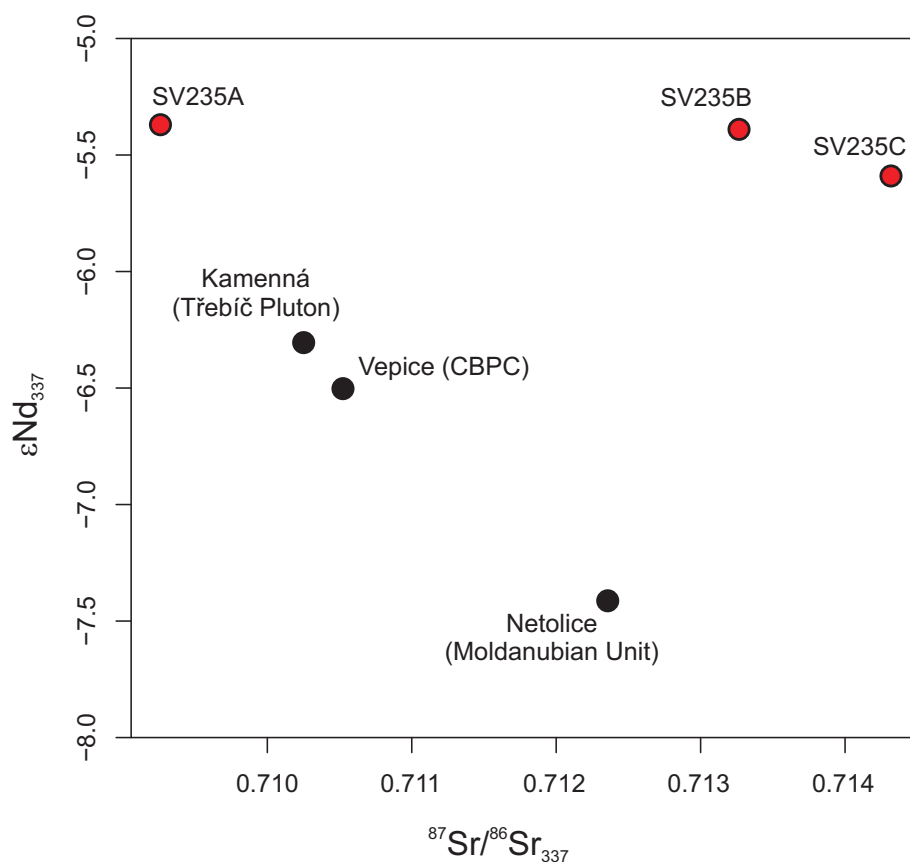


Fig. 9 The binary plot $^{87}\text{Sr}/^{86}\text{Sr}_{337}$ versus ϵNd_{337} . The diagram contains representative analyses for durbachites from the Central Bohemian Plutonic Complex (CBPC), Moldanubian Unit and Třebíč Pluton after Holub and Janoušek (2003) recalculated to 337 Ma.

Tab. 6 (Present-day) Re–Os isotopic data for phlogopite pyroxenites

Sample	Re (ppb)	Os (ppb)	Re/Os	$^{187}\text{Re}/^{188}\text{Os}$	$^{187}\text{Os}/^{188}\text{Os}$	2 SE	γOs	T_{MA} (Ma) PUM
SV235A	1.62	0.076	21.3	107	0.4622	7	257	187
SV235C	2.96	0.070	42.3	236	1.3230	6	921	304

The radiogenic ratios of $^{187}\text{Os}/^{188}\text{Os}$ (0.4622 and 1.3230), low content of Os (0.076 and 0.070 ppb) and elevated concentrations of Re (1.62 and 2.96 ppb) in the two whole-rock samples all indicate crustal origin of the sulphides (e.g., Aulbach et al. 2010). On the other hand, initial $^{187}\text{Os}/^{188}\text{Os}$ ratios are confusing because probably the system was open during the origin of sulphides. Crystal lattice of sulphides, in particular of pyrrhotite, should play a key role in poor Os retention (e.g., Morelli et al. 2010).

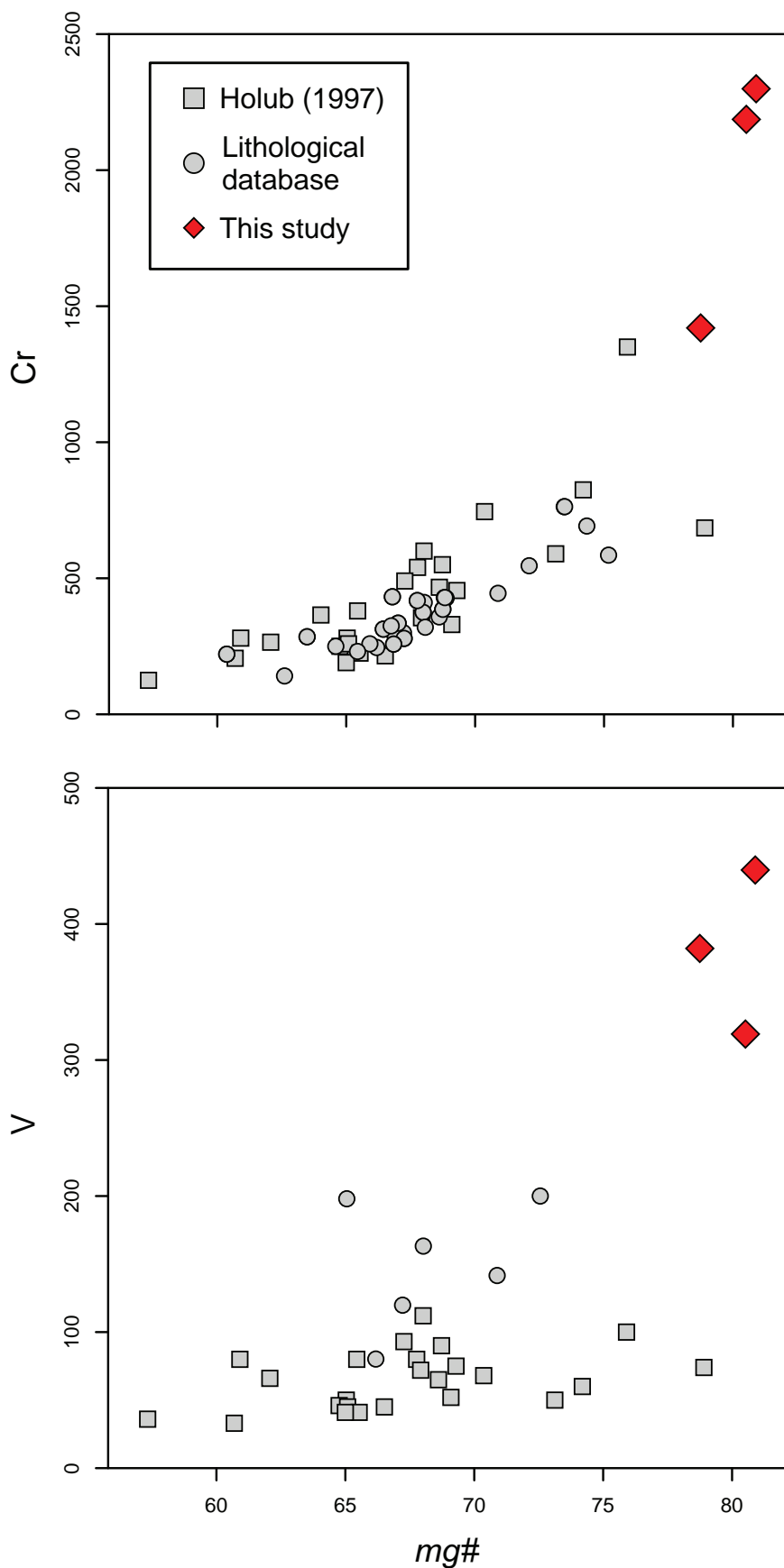
The best match in the Sr–Nd isotopic compositions of phlogopite pyroxenites ($^{87}\text{Sr}/^{86}\text{Sr}_{340}$ 0.7093–0.7143; ϵNd_{340}

between –5.4 and –5.6) is observed in some durbachites in the Central Bohemian Plutonic Complex (Vepice; $^{87}\text{Sr}/^{86}\text{Sr}_{337}$ = 0.71048; ϵNd_{337} –6.5), the Moldanubian Zone (Netolice; $^{87}\text{Sr}/^{86}\text{Sr}_{337}$ = 0.7125; ϵNd_{337} –7.4) and Třebíč Pluton (Kamenná; $^{87}\text{Sr}/^{86}\text{Sr}_{337}$ = 0.71026; ϵNd_{337} –6.3) (Holub and Janoušek 2003) (Fig. 9).

A review of geothermometry estimates for durbachitic granitoids (Holub 1997) indicates values ranging from 740 °C for mafic facies of the Milevsko Massif (K-feldspar–biotite thermometry, Minařík and Povondra 1976). Higher temperature estimates of 750–850 °C were obtained by Hejtman (1975) for dioritic

Tab. 7 Equilibration temperatures for selected mineral compositions of pyroxenes and phlogopite

assumed pressure (kbar)	method	reference	T (°C)
3	two-pyroxene	Bertrand and Mercier (1985)	999
	two-pyroxene	Brey and Köhler (1990)	969
	two-pyroxene	Taylor (1998)	1 038
3	Ca-in-Opx	Brey and Köhler (1990)	917
surface pressure	coupled exchange of Ti and Fe^{2+} in biotite	Luhr et al. (1984)	1 007



to amphibole–phlogopite-rich ultramafic durbachite-related types in the Prachatice area. Application of two-pyroxene thermometer of Wells (1977) by Holub (1997) on pyroxene-bearing rocks near Písek, southern Bohemia, yielded temperatures of 900–950 °C. This comparison for durbachites and related ultramafic rocks indicates a range of temperatures from the best-preserved two-pyroxene phlogopite pyroxenite, as exemplified by the Přední Zvonková body (c. 1000 °C), to approximately 750 °C for granitoid durbachites.

5.2. Tectonic position of phlogopite pyroxenite and possible relations to durbachite bodies

The sample A in this study represents a phlogopite pyroxenite (ultramafic durbachite rock) with preserved fresh orthopyroxene besides diopside. It stands in contrast to 31 small intrusions in the Prachatice Granulite Massif, which contain amphibole in place of pyroxenes (Hejtman 1975).

The occurrence of phlogopite pyroxenite cumulate with minor diopside pyroxenite layers could be interpreted as an *in situ* example of crustal domain in which accumulation of crystals took place in a local magma chamber. In this context small durbachite intrusions to the west in the Smrčiny area and especially the medium-size Knížecí Stolec Pluton 8 km to the north are of interest (Fig. 1), as they seem to represent possibly different crustal levels than the phlogopite pyroxenite. These relations suggest possible role of vertical displacements of individual structural segments on late shear zones and faults (Beneš et al. 1983, Vrána and Šrámek 1999;

Fig. 10 Variation diagrams of Cr and V (ppm) in studied phlogopite pyroxenites and durbachitide rocks from the Moldanubian Zone of the Bohemian Massif.

Verner et al. 2008), connected mainly with a relatively late regional deformation event D_3 (Vrána and Šrámek 1999) and later normal faulting. This seems to be important as the occurrence of ultramafic cumulate marks a level of crystal settling.

Taken together, the evolution of phlogopite pyroxenite probably included the following steps: (i) Formation of a hybrid magma by mixing upper mantle-derived and leucogranite melt components; (ii) Fractional crystallization and accumulation of phlogopite and pyroxenes (plus apatite and sulphides) in proportions corresponding to sample A; (iii) Relative tectonic movements of local crustal segments along late structures.

6. Conclusions

- Phlogopite pyroxenite, found during field assessment of geophysical anomalies near the Přední Zvonková village in the Šumava/Bohemian Forest (Böhmerwald) region (Czech Republic), exhibits geochemical and petrological relations with durbachites. The euhedral/subhedral shape of pyroxenes, presence of diopside-enriched bands, a strong enrichment in apatite and segregation of sulphides suggesting melt immiscibility, all accentuate the character of phlogopite pyroxenites as crystal cumulates.
- Although the studied phlogopite pyroxenites have ultramafic composition, they evolved by fractional crystallization/accumulation from a hybrid durbachitic melt. The phlogopite pyroxenite geochemistry cannot be explained without incorporation of a granitic crustal component.
- Sr–Nd isotope geochemistry, as well as Re–Os isotopes, indicates a prolonged crustal residence of crustal material prior to its incorporation into the durbachitic magma.
- Two-pyroxene thermometry of sample SV235A, using three calculation procedures, yields values 970–1040 °C. The low Zr contents in pyroxenites (56–95 ppm) and lack of zircon suggest that the crystallization temperature was well above the zircon saturation temperature.
- Whereas most published durbachite studies accentuate the aspect of mixing of an upper mantle-derived melt with a crustal melt of approximately granitic composition and others are oriented to the role of fractional crystallization, our results argue for combined role of both processes. The ultramafic phlogopite pyroxenite from Přední Zvonková is not an example of a simple, Mg-rich upper mantle component.
- The relatively late tectonic disintegration of these parts of the Moldanubian Complex into a mosaic of mutually displaced segments (mainly D_3 event and later

normal faulting) resulted in an exposure of contrasting levels of durbachitic plutonism. For this reason are encountered examples of “in situ” high-T ultramafic crystal cumulates, as well as plutonic masses of crystallized granitoid durbachites at the present level of erosion.

Acknowledgements. We thank the chief editor Vojtěch Janoušek and both reviewers František Holub and Lukáš Krmíček for their suggestions resulting in improvement of the text. Assistance of Josef Šrámek in completing the gravimetric and magnetometric data is greatly acknowledged. We are also indebted to Vojtěch Erban (Czech Geological Survey) for the help with TIMS measurement of Sr and Re–Os isotopes and Jitka Míková with MC-ICP-MS determination of Nd isotopes. We thank Petr Gadas (Masaryk University, Brno) for the electron-microprobe work. The study was supported by the Project 390002 of the Czech Geological Survey, Charles University Operational Programme OPPK CZ.2.16/3.1.00/21516) and Grant-in-aid internal program of international cooperation projects of the Czech Academy of Science (No. M100131203) and the Scientific Programme RVO67985831 of the Institute of Geology v.v.i of the Czech Academy of Sciences.

References

- AULBACH S, KRAUSS C, CREASER, RA, STACHEL T, HEAMAN LM, MATVEEV S, CHACKO T (2010) Granulite sulphides as tracers of lower crustal origin and evolution: an example from the Slave Craton, Canada. *Geochim Cosmochim Acta* 74: 5368–5381
- BENEŠ K, HOLUBEC J, SURŇÁKOVÁ R, ZEMAN J (1983) Geological structure of the Moldanubicum in the Bohemian Forest area. *Rozpr Čs Akad Věd, Ř mat příř Věd* 93: 1–68 (in Czech)
- BERTRAND P, MERCIER J-CC (1985) The mutual solubility of coexisting ortho- and clinopyroxene: toward an absolute geothermometer for the natural system? *Earth Planet Sci Lett* 76: 109–122
- BIRCK JL, BARMAN MR, CAPMAS F (1997) Re–Os isotopic measurements at the femtomole level in natural samples. *Geostand Newsl* 21: 19–27
- BOYNTON WV (1984) Cosmochemistry of the rare earth elements: meteorite studies. In: HENDERSON P (ed) *Rare Earth Element Geochemistry*. Elsevier, Amsterdam, pp 63–114
- BREITER K (2008) Durbachites of the Třebíč pluton – genetic implications. *Zpr geol Výzk v Roce 2007*: 143–147 (in Czech with English abstract)
- BREITER K, KOLLER F (2009) Mafic K- and Mg-rich magmatic rocks from Western Mühlviertel (Austria) area and the

- adjacent part of the Šumava Mountains (Czech Republic). *Jb Geol B–A* 149: 477–485
- BREY GP, KÖHLER T (1990) Geothermobarometry in four-phase lherzolites. II. New thermobarometers and practical assessment of existing thermobarometers. *J Petrol* 31: 1352–1378
- COHEN AS, WATERS FG (1996) Separation of osmium from geological materials by solvent extraction for analysis by thermal ionisation mass spectrometry. *Anal Chim Acta* 332: 269–275
- COX KG, BELL JD, PANKHURST RJ (1979) *The Interpretation of Igneous Rocks*. Allen & Unwin, London, pp 1–464
- DALLMEYER RD, FRANKE W, WEBER K (eds) (1995) *Pre-Permian Geology of Central and Eastern Europe*. Springer-Verlag, Berlin, pp 1–611
- DEMPÍROVÁ L (2010) The evaluation of precision and relative error of the main components of silicate analyses in Central Laboratory of the CGS. *Zpr geol Výzk v Roce 2009*: 326–330 (in Czech)
- FIALA J, FUCHS G, WENDT JI (1995) Stratigraphy of the Moldanubian Zone. In: DALLMEYER RD, FRANKE W, WEBER K (eds) *Pre-Permian Geology of Central and Eastern Europe*. Springer-Verlag, Berlin, pp 417–428
- FOLEY SF, VENTURELLI G, GREEN DH, TOSCANI L (1987) The ultrapotassic rocks: characteristics, classification, and constraints for petrogenetic models. *Earth Sci Rev* 24: 81–134
- GERDES A, WÖRNER G, FINGER F (2000) Hybrids, magma mixing and enriched mantle melts in post-collisional Variscan granitoids: the Rastenberg Pluton, Austria. In: FRANKE W, HAAK V, ONCKEN O, TANNER D (eds) *Orogenic Processes: Quantification and Modelling in the Variscan Fold Belt*. Geological Society London Special Publications 179: pp 415–431
- GÜRTLEROVÁ P, ČADEK J, ČADKOVA Z, MRÁZEK P, ADAMOVÁ M, DUŠEK P (1997) Database of analytical determinations on maps of rock geochemical reactivity 1 : 50 000. In: *Litho-geochemical Database of the Czech Geological Survey*, Prague
- HEJTMAN B (1975) Biotitites and associated plutonic rocks in the Prachatice granulite body and its vicinity. *Acta Univ Carol, Geol*: 265–300
- HOLUB F (1997) Ultrapotassic plutonic rocks of the durbachite series in the Bohemian Massif: petrology, geochemistry and petrogenetic interpretation. *Sbor geol Věd, ložisk Geol Mineral*. 31: 5–26
- HOLUB FV, JANOUŠEK V (2003) Geochemical and Sr–Nd isotopic constraints on the genesis of ultrapotassic plutonic rocks from the Moldanubian Zone of the Bohemian Massif. *J Geosci* 48: 61–62
- JACOBSEN SB, WASSERBURG GJ (1980) Sm–Nd isotopic evolution of chondrites. *Earth Planet Sci Lett* 50: 139–155
- JANOUŠEK V, HOLUB FV (2007) The causal link between HP–HT metamorphism and ultrapotassic magmatism in collisional orogens: case study from the Moldanubian Zone of the Bohemian Massif. *Proc Geol Assoc* 118: 75–86
- JANOUŠEK V, FARROW CM, ERBAN V (2006) Interpretation of whole-rock geochemical data in igneous geochemistry: introducing Geochemical Data Toolkit (GCDkit). *J Petrol* 47: 1255–1259
- JANOUŠEK V, FARROW CM, ERBAN V, TRUBAČ J (2011) Brand new Geochemical Data Toolkit (GCDkit 3.0) – is it worth upgrading and browsing documentation? (Yes!). *Geol výzk Mor Slez* 18: 26–30
- KOŠLER J, KONOPÁSEK J, SLÁMA J, VRÁNA S (2013) U–Pb zircon provenance of Moldanubian metasediments in the Bohemian Massif. *J Geol Soc, London* 171: 83–95
- LE MAITRE RW (ed), STRECKEISEN A, ZANETTIN B, LE BAS MJ, BONIN B, BATEMAN P, BELLIENI G, DUDEK A, EFREMOVA S, KELLER J, LAMEYRE J, SABINE, PA, SCHMID, R, SØRENSEN, H, WOOLLEY AR (2002) *Igneous Rocks. A Classification and Glossary of Terms, 2nd Edition*. Cambridge University Press, Cambridge, pp 1–236
- LEAKE BE, WOOLLEY AR, BIRCH WD, BURKE EAJ, FERRARIS G, GRICE JD, HAWTHORNE FC, KISCH HJ, KRIVOVICHEV VG, SCHUMACHER JC, STEPHENSON NCN, WHITTAKER EJW (2003) Nomenclature of amphiboles: additions and revisions to the International Mineralogical Association’s 1997 Recommendations. *Canad Mineral* 41: 1355–1362
- LIEW TC, HOFMANN AW (1988) Precambrian crustal components, plutonic associations, plate environment of the Hercynian Fold Belt of Central Europe: indications from Nd and Sr isotopic study. *Contrib Mineral Petrol* 98: 129–138
- LUGMAIR GW, MARTI K (1978) Lunar initial ¹⁴³Nd/¹⁴⁴Nd: differential evolution line of the lunar crust and mantle. *Earth Planet Sci Lett* 39: 349–357
- LUHR JF, CARMICHAEL ISE, VAREKAMP JC (1984) The 1982 eruptions of El Chichón volcano, Chiapas, Mexico: mineralogy and petrology of the anhydrite-bearing pumices. *J Volcanol Geotherm Res* 23: 69–108
- MCCANN T (2008) *The Geology of Central Europe. Volume 1: Precambrian and Palaeozoic*. The Geological Society, London, pp 1–784
- MEISEL T, WALKER RJ, IRVING AJ, LORAND J-P (2001) Osmium isotopic compositions of mantle xenoliths: a global perspective. *Geochim Cosmochim Acta* 65: 1311–1323
- MÍKOVÁ J, DENKOVÁ P (2007) Modified chromatographic separation scheme for Sr and Nd isotope analysis in geological silicate samples. *J Geosci* 52: 221–226
- MINAŘÍK L, POVONDRA P (1976) Geochemistry of potassium feldspars from the durbachites of the Čertovo břemeno type. *Stud ČSAV* 9: 1–63
- MORELLI RM, BELL CC, CREASER RA, SIMONETTI A (2010) Constraints on the genesis of gold mineralization at the Homestake Gold Deposit, Black Hills, South Dakota from rhenium–osmium sulphide geochronology. *Miner Depos* 45: 461–480
- PARAT F, HOLTZ F, RENÉ M, ALMEEV R (2010) Experimental constraints on ultrapotassic magmatism from the Bohe-

- mian Massif (durbachite series, Czech Republic). *Contrib Mineral Petrol* 159: 331–347
- PIN C, ZALDUEGUI JFS (1997) Sequential separation of light rare-earth elements, thorium and uranium by miniaturized extraction chromatography: application to isotopic analyses of silicate rocks. *Anal Chim Acta* 339: 79–89
- PIN C, BRIOT D, BASSIN C, POITRASSON F (1994) Concomitant separation of strontium and samarium–neodymium for isotopic analysis in silicate samples, based on specific extraction chromatography. *Anal Chim Acta* 298: 209–217
- POUCHOU JL, PICOIR F (1985) “PAP” (ϕ - ρ - Z) procedure for improved quantitative microanalysis. In: ARMSTRONG JT (ed) *Microbeam Analysis*. San Francisco Press, pp 104–106
- SHIREY SB, WALKER RJ (1998) The Re–Os isotope system in cosmochemistry and high-temperature geochemistry. *Ann Rev Earth Planet Sci* 26: 423–500
- SCHULMANN K, KONOPÁSEK J, JANOUŠEK V, LEXA O, LARDEAUX JM, EDEL JB, ŠTÍPSKÁ P, ULRICH S (2009) An Andean type Palaeozoic convergence in the Bohemian Massif. *C R Geosci* 341: 266–286
- SMOLIAR MI, WALKER RJ, MORGAN JW (1996) Re–Os isotope constraints on the age of Group IIA, IIIA, IVA, and IVB iron meteorites. *Science* 271: 1099–1102
- STEIGER RH, JÄGER E (1977) Subcommittee on Geochronology; convention on the use of decay constants in geo- and cosmochronology. *Earth Planet Sci Lett* 36: 359–362
- ŠALANSKÝ K, MANOVÁ M, RACKOVÁ H (1988) Explanation to Geophysical Map 1:25 000, Sheet 32-233 Černá v Pošumaví. Unpublished manuscript, Czech Geological Survey, Prague, pp 1–21
- ŠRÁMEK J (2010) Geophysics. In: VRÁNA S (ed) Explanation to Geological Map of the Czech Republic 1:25 000, Sheet 32-233 Černá v Pošumaví. Czech Geological Survey, Prague, pp 37–42 (in Czech)
- TABAUD AS, JANOUŠEK V, SKRZYPEK E, SCHULMANN K, ROSSI P, WHITECHURCH H, GUERROT C, PAQUETTE JL (2015) Chronology, petrogenesis and heat sources for successive Carboniferous magmatic events in the southern-central Variscan Vosges Mts. (NE France). *J Geol Soc, London* 172: 87–102
- TANAKA T, TOGASHI S, KAMIOKA H, AMAKAWA H, KAGAMI H, HAMAMOTO T, YUHARA M, ORIHASHI Y, YONEDA S, SHIMIZU H, KUNIMARU T, TAKAHASHI K, YANAGI T, NAKANO T, FUJIMAKI H, SHINJO R, ASAHARA Y, TANIMIZU M, DRAGUSANU C (2000) JNdi-1: a neodymium isotopic reference in consistency with La Jolla neodymium. *Chem Geol* 168: 279–281
- TAYLOR SR, McLENNAN SM (1995) The geochemical evolution of the continental crust. *Rev Geophys* 33: 241–265
- TAYLOR WR (1998) An experimental test of some geothermometer and geobarometer formulations for upper mantle peridotites with application to the thermobarometry of fertile lherzolite and garnet websterite. *Neu Jb Mineral, Abh* 172: 381–408
- TINDLE A (2015) Mineral recalculation software. Accessed on March 16, 2015, at <http://www.open.ac.uk/earth-research/tindle/AGTWebPages/AGTSoft.html>
- VERNER K, ŽÁK J, NAHODILOVÁ R, HOLUB FV (2008) Magmatic fabrics and emplacement of the cone-sheet-bearing Knížecí Stolec durbachite pluton (Moldanubian Unit, Bohemian Massif): implications for mid-crustal reworking of granulitic lower crust in the Central European Variscides. *Int J Earth Sci* 97: 19–33
- VON RAUMER JF, FINGER F, VESELÁ P, STAMPFLI GM (2014) Durbachites–vaugnerites – a geodynamic marker in the central European Variscan orogen. *Terra Nova* 26: 85–95
- VRÁNA S, ŠRÁMEK J (1999) Geological interpretation of detailed gravity survey of the granulite complex in southern Bohemia and its structure. *Bull Czech Geol Survey* 74: 261–277
- VRÁNA S, BLÜMEL P, PETRAKAKIS K (1995) Moldanubian Zone: metamorphic evolution. In: DALLMEYER D, FRANKE W, WEBER K (eds) *Pre-Permian Geology of the Central and Western Europe*. Springer-Verlag, Berlin, pp 453–466
- VRÁNA S, BRÍZOVÁ E, DVOŘÁK I, GRUNDLOCH J, HOLÁSEK O, KADLECOVÁ R, KREJČÍ Z, KRUPÍČKA J, LYSENKO V, MANOVÁ M, NÝVLT D, POŇAVIČ M, PŘECHOVÁ E, ŠRÁMEK J, TRUBAČ J, VERNER K (2010) Explanation to Geological Map of the Czech Republic 1:25 000, Sheet 32-233 Černá v Pošumaví. Unpublished manuscript, Czech Geological Survey, Prague, pp 1–125 (in Czech)
- WASSERBURG GJ, JACOBSEN SB, DEPAOLO DJ, McCULLOCH MT, WEN T (1981) Precise determination of Sm/Nd ratios, Sm and Nd isotopic abundances in standard solutions. *Geochim Cosmochim Acta* 45: 2311–2324
- WELLS PR (1977) Pyroxene thermometry in simple and complex systems. *Contrib Mineral Petrol* 62: 129–139
- WHITNEY DL, EVANS BW (2010) Abbreviations for names of rock-forming minerals. *Amer Miner* 95: 185–187
- ŽÁK J, VERNER K, JANOUŠEK V, HOLUB FV, KACHLÍK V, FINGER F, HAJNÁ J, TOMEK F, VONDRŮVÍČ L, TRUBAČ J (2014) A plate-kinematic model for the assembly of the Bohemian Massif constrained by structural relationships around granitoid plutons. In: SCHULMANN K, MARTÍNEZ CATALÁN JR, LARDEAUX JM, JANOUŠEK V, OGGIANO G (eds) *The Variscan Orogeny: Extent, Timescale and the Formation of the European Crust*. Geological Society London Special Publications 405: pp 169–196

